Celestial objects as strongly-interacting nonannihilating dark matter detectors

Anupam Ray*

Department of Physics, University of California Berkeley, Berkeley, California 94720, USA and School of Physics and Astronomy, University of Minnesota, Minneapolis, Minnesota 55455, USA

(Received 10 January 2023; accepted 9 March 2023; published 7 April 2023)

Nonannihilating dark matter particles, owing to their interactions with ordinary baryonic matter, can efficiently accumulate inside celestial objects. For heavy mass, they gravitate toward the core of the celestial objects, thermalize in a small core region, and eventually form tiny black holes via core collapse, resulting destruction of the host objects. We demonstrate that the existence of a variety of celestial objects provides stringent constraints on strongly interacting heavy dark matter, a blind spot for the terrestrial dark matter detectors as well as for the cosmological probes. Celestial objects with larger sizes and lower core temperatures, such as Jupiter, are the most optimal detectors to probe the strongly interacting heavy nonannihilating dark matter.

DOI: 10.1103/PhysRevD.107.083012

I. INTRODUCTION

The existence of dark matter (DM) has been firmly established through its gravitational interactions with the ordinary baryonic matter [1]. However, its identity still remains a mystery. The ongoing terrestrial and cosmological searches are trying to pinpoint its mass and hypothesized non gravitational interactions with the baryonic matter [2,3]. While some DM parameters have been excluded by these searches, many well-motivated candidates are yet to be explored. Strongly interacting heavy nonannihilating DM is one such regime that remains largely untested.

In this work, we demonstrate that celestial objects are excellent laboratories to search for strongly interacting heavy nonannihilating DM. More specifically, we point out that the continued existence of a variety of stellar objects provides stringent exclusions on nonannihilating DM interactions over a wide mass range. We mainly answer two basic questions: Why are celestial objects superior to search for strongly interacting heavy nonannihilating DM as compared to the terrestrial detectors? Which celestial objects are the most optimal targets?

Traditional direct detection experiments are not well suited for heavy DM searches. The flux of Galactic DM at terrestrial detectors falls off linearly with higher DM mass, and the constraints weaken accordingly. Whereas, because of the enormous sizes of astrophysical objects and their long lifetimes, the effective exposure time ($\sim M_\odot\,\mathrm{Gyr}$) is orders of magnitude larger than human-made direct detection experiments ($\sim$kT yr), naturally providing sensitivity to the tiny flux of heavy DM.

Strongly interacting DM is yet another blind spot for typical direct detection experiments. If DM particles interact too strongly with baryonic matter, then they lose a significant fraction of their energies via interactions with the material in the atmosphere as well as in the Earth-cover above the underground detectors. As a consequence, they slow down significantly and can not deposit sufficient amounts of energy for detection. Whereas, stellar objects are ideal probes for strongly interacting DM as almost all the DM particles that transit through the stellar objects get trapped, leading to a maximal sensitivity.

Accumulation of particle DM in celestial objects is a key astrophysical probe of non gravitational interactions of DM with the ordinary baryonic matter. DM particles from the galactic halo, owing to their interactions with the stellar constituents, can downscatter to energies below the local escape energy, and become gravitationally bound to the stellar objects [4–6]. These bound DM particles lose more energy via repeated scatterings with the stellar constituents and eventually thermalize inside the stellar volume. Such bound thermalized DM particles can become abundant inside the stellar volume if they have sufficiently strong interactions with the baryonic matter and possess intriguing phenomenological signatures.

For nonannihilating DM, such bound DM particles gradually accumulate, and for heavy DM masses, they settle in a small region around the stellar core. Because of their prodigious abundance in a tiny core volume, their

*anupam.ray@berkeley.edu

number density within the stellar core becomes quite large, allowing dark core collapse and subsequent black hole (BH) formation. This nascent BH, if not too light, can rapidly swallow the host, and the existence of stellar objects provides stringent constraints on nonannihilating DM interactions.

This scenario has been extensively studied in the context of old neutron stars [7–28] primarily because of their enormously large baryonic density as well as high compactness. More specifically, neutron stars can capture a significant number of DM particles from the Galactic halo even for the low DM-nucleon scattering cross sections as the single-collision capture rate scales linearly with the compactness $(\sim M/R)$. Quantitatively, for a solar mass neutron star, residing in the solar neighborhood, with a typical radius of 10 km, the capture rate is $\mathcal{O}(10^5)$ times larger than the Sun for low DM interactions. Apart from that, because of their large baryonic density $(\sim M/R^3)$, the accumulated DM particles thermalize in a tiny region around the core, implying a huge core-density favorable for transmutation. This indicates neutron stars are the most optimal targets to probe weakly interacting heavy nonannihilating DM, and the existence of old neutron stars in the solar neighborhood excludes $m_\chi = 10^6$ GeV and $\sigma_{\chi n} = 10^{-48}$ cm^2, the leading constraints on nonannihilating DM interactions [11,20].

However, in the optically thick (large DM-nucleon scattering cross section) regime, noncompact objects such as the Sun, Jupiter, and Earth are more suitable detectors to probe nonannihilating DM interactions. This is simply because in the optically thick regime, almost all of the DM particles that transit through a stellar object get trapped, and therefore, the accumulation rate increases with the larger size. Since the noncompact objects possess much larger radii, the accumulation rate for noncompact objects becomes comparable or even larger than the neutron stars in the strongly interacting regime. Quantitatively, for $m_\chi = 10^6$ GeV, and sufficiently high $\sigma_{\chi n}$, the transit (accumulation) rate for a typical neutron star, residing in the solar neighborhood, is 10^{19} s^{-1}, comparable to the Earth, and 10^{-2} (10^{-5}) smaller than the Jupiter (Sun). This naturally motivates us to explore the potential of noncompact stellar objects as strongly interacting nonannihilating DM detectors. We found that stellar objects with relatively large radii and low core temperature (such as Jupiter) are the most optimal detectors. This is simply because the total number of accumulated DM particles increases with a larger radius, and the BH formation becomes easier with a lower core temperature, implying the most favorable transmutation criterion. Prior works [29–31], more particularly Ref. [31], have recently explored the transmutation scenario for the Earth and the Sun. We systematically revisit the issue to gain more insight on the constraints, and we show that stellar objects with larger sizes and small core temperatures, such as Jupiter, provide the leading constraints on strongly interacting heavy nonannihilating DM (see also Refs. [32,33] for probing annihilating DM interactions with Jupiter-like planets).

The rest of the paper is organized as follows. In Sec. II, we discuss different stages of DM-induced collapse of the celestial objects. In Sec. III, we present our exclusion limits from the existence of several stellar objects, demonstrating that the constraints obtained in this analysis cover new parts of the DM parameter space and bridge the gap between the cosmological probes [34–37] and the terrestrial detectors [38–42]. Finally, we summarize and conclude in Sec. IV.

II. DARK MATTER INDUCED COLLAPSE OF STELLAR OBJECTS

Nonannihilating DM particles can accumulate efficiently inside the stellar volume if they possess sufficiently strong interactions with the stellar nuclei. For heavy DM mass, they gravitate towards the stellar core and settle in a tiny core region. Because of their prodigious abundance, and tiny core volume, their number density within the stellar core becomes tantalizingly larger, eventually resulting in a BH formation inside the stellar core. This nascent BH, if not sufficiently light, can rapidly swallow the host, transmuting them to comparable mass BHs. In the following, we discuss different stages of DM-induced collapse of stellar objects, and a schematic diagram for this process is depicted in Fig. 1.

A. Dark matter accumulation

We first estimate the total number of captured DM particles inside the stellar volume. For clarity, we define the maximal capture rate as saturation capture rate $(C_{\rm sat})$, and it occurs when all of the DM particles that transit through the stellar objects get trapped. For a particular velocity distribution of the incoming DM particles, the saturation capture rate is [6]

$$C_{\rm sat} = \frac{\rho_\chi}{m_\chi}\pi R^2 \int \frac{f(u)du}{u}(u^2 + v_{\rm esc}^2), \tag{1}$$

where $\rho_\chi = 0.4$ GeV/cm^3 is the Galactic DM density, m_χ is the DM mass, and R is the radius of the stellar object. $f(u)$ denotes the velocity distribution of the incoming DM particles, with $v_{\rm esc}$ being the escape velocity of the stellar objects. For a Maxwell-Boltzmann velocity distribution, $C_{\rm sat}$ simplifies to

$$C_{\rm sat} = \frac{\rho_\chi}{m_\chi}\pi R^2 \sqrt{\frac{8}{3\pi}}\bar{v}\left(1 + \frac{3v_{\rm esc}^2}{2\bar{v}^2}\right), \tag{2}$$

where $\bar{v} = 270$ km/s denotes the average velocity of the DM particles in the Galactic halo.

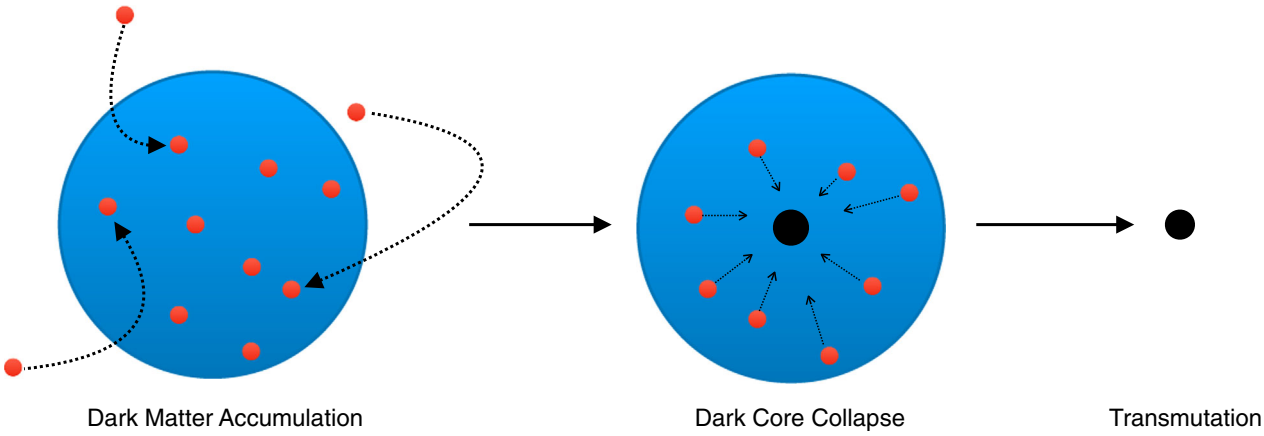

FIG. 1. Transmutation of stellar objects via gradual accumulation of nonannihilating DM. Heavy DM gravitate towards the core of the stellar objects and form tiny black holes via dark core collapse. These nascent BHs rapidly transmute the hosts by swallowing them, resulting in comparable low mass BHs.

A certain fraction of the DM particles will be captured by interacting with the stellar constituents, and we aim to estimate this capture fraction (f_c). Since we are mostly interested in the optically thick regime (large DM-nucleon scattering cross section), f_c behaves differently for heavier and lighter DM. For heavier DM, i.e., when the DM mass (m_χ) is larger than the target mass (m_A), scatterings do not alter the direction of the incoming DM particles. As a consequence, the trajectories of the incoming DM particles are not randomized, and they follow almost a linear trajectory that ends inside the stellar interior when the final velocity falls below the escape velocity. In this case, in the limit of multiple collisions, the DM particles are essentially guaranteed to be captured, resulting in $f_c = 1$ [43]. Whereas, in the opposite regime $(m_\chi < m_A)$, the direction of the DM particles gets randomized after each collision, and, as a result, a certain fraction of the DM particles can always escape from the stellar volume via reflection. This implies that for lighter DM, even for arbitrarily large cross sections, the capture rate never reaches its saturation value $(f_c < 1)$ [43].

For this analysis, we are interested in heavy DM capture inside stellar objects, and hence, we take $f_c = 1$. It implies that, in the optically thick regime, we take the capture rate to its saturation value, and it does not depend on the DM-nucleon scattering cross section. For light DM capture in celestial objects, f_c can be determined by the recent MCMC results [43], or from analytical estimates [44], both of which agree reasonably well.

In the optically thin regime (small DM-nucleon scattering cross section), capture occurs via single scattering. This is simply because for smaller values of DM-nucleon scattering cross sections, the mean free path of the incoming DM particles becomes larger and becomes comparable to the size of the stellar objects, and, as a result, they scatter once while transiting through the host. For this regime, we use the single-collision capture treatment [6], and f_c becomes substantially smaller.

B. Spatial distribution of dark matter inside stellar objects

Captured DM particles rapidly thermalize inside the celestial objects for sufficiently high DM-nuclei scattering cross sections [11–13,20,31,45,46], and the spatial distribution of the thermalized DM particles inside the stellar volume depends on the effects of diffusion and gravity [47–49]. By considering the effects of diffusion and gravity in a self-consistent manner, the spatial distribution of the thermalized DM particles is [49]

$$\frac{\nabla n_\chi(r)}{n_\chi(r)} + (\kappa+1)\frac{\nabla T(r)}{T(r)} + \frac{m_\chi g(r)}{T(r)} = \frac{\Phi}{n_\chi(r) D_{\chi n}(r)}\frac{R_\oplus^2}{r^2}, \tag{3}$$

where $n_\chi(r)$ denotes the number density of the thermalized DM particles within the stellar volume. $T(r)$ denotes the temperature profile of the celestial objects, and $\Phi = C/\pi R_\oplus^2$ is the incoming flux of the DM particles, with C denotes the capture rate. $\kappa \sim -1/[2(1+m_\chi/m_A)^{3/2}]$ and $D_{\chi n} \sim \lambda v_{\rm th}$ are the diffusion coefficients, where λ denotes the mean free path of the DM particles and $v_{\rm th}$ denotes their thermal velocity. It is evident that, for very heavy DM mass, the diffusion coefficient (κ) becomes smaller as it scales as $m_\chi^{-3/2}$, and gravity (scales proportional to m_χ) dominates over the diffusion processes. Therefore, heavy DM tends to settle down towards the core of the stellar objects. Quantitatively, by solving Eq. (3) for $n_\chi(r)$ with the boundary condition that the volume integral of $n_\chi(r)$ provides the total number of captured DM particles, one can demonstrate that the captured DM particles mostly concentrate around the stellar core if they are heavy [49].

Concentration of heavy DM around the stellar core can also be explained from the radius of the thermalization sphere ($r_{\rm th} = \sqrt{9k_BT/(4\pi G\rho m_\chi)}$), which results from the balance between the thermal pressure and the gravitational potential [11,12]. Since, the radius of the thermalization sphere scales as $m_\chi^{-1/2}$, for heavy DM, $r_{\rm th}$ becomes smaller, indicating that the concentration of the captured DM particles primarily occurs around the core.

C. Dark core collapse and black hole formation

For nonannihilating DM, accumulation grows linearly in time. As a consequence, the number density of the captured DM particles inside the thermalization volume becomes tantalizingly large. Quantitatively, for DM mass of 10^6 GeV, and sufficiently high DM-nuclei scattering cross section (say 10^{-28} cm^2), $\mathcal{O}(10^{36})$ number of DM particles thermalize inside the Earth within a radius of $\sim$6 km, indicating a number density of $\sim 2\times 10^{18}$ cm^{-3}. This corresponds to a core density of $\sim 2\times 10^{24}$ GeV cm^{-3}, around 25 orders of magnitude higher than the local Galactic DM density, and it further increases as $m_\chi^{3/2}$ for heavier DM masses. Once the core density exceeds its critical threshold value, it undergoes a gravitational collapse, and eventually results in a BH formation inside the stellar core [7–24,31]. In the following, we quantify the critical core density for the stellar objects.

The BH formation criterion via dark core collapse has been extensively discussed in the literature for compact stars [7–24,26–28,31], and is essentially determined by two conditions. The first one is within the stable thermal radius, the DM density has to exceed the corresponding baryonic density (ρ_b). It leads to a self-gravitational collapse of the thermalized DM particles and is determined by [11,13,20]

$$\frac{m_\chi N_\chi^{\rm self}}{\frac{4}{3}\pi r_{\rm th}^3} \geq \rho_b, \tag{4}$$

where $N_\chi^{\rm self}$ denotes the critical number of DM particles for ensuing self-gravitating collapse.[1] It is independent of the spin of the DM particles and only depends on the DM mass as well as properties of the stellar objects such as core density and core temperature. For Earth, it corresponds to

$$N_\chi^{\rm self} \sim 7\times 10^{36}\left(\frac{\rho_{\rm core}}{13\ {\rm g/cm^3}}\right)\left(\frac{T_{\rm core}}{5800\ {\rm K}}\right)^{3/2}\left(\frac{10^7\ {\rm GeV}}{m_\chi}\right)^{5/2}, \tag{5}$$

where, $\rho_{\rm core}$ denotes the core density, and $T_{\rm core}$ denotes the core temperature. The second condition is determined by the maximum number of DM particles that can be stabilized by the quantum degeneracy pressure and is commonly known as Chandrasekhar limit ($N_\chi^{\rm cha}$). Chandrasekhar limit depends on the spin statistics of the DM particles as the quantum degeneracy pressure for bosonic DM stems from the uncertainty principle, whereas, for fermionic DM, it arises from the Pauli exclusion principle. $N_\chi^{\rm cha}$ solely depends on the DM mass and for bosonic (fermionic) DM, it corresponds to $M_{\rm pl}^2/m_\chi^2 (M_{\rm pl}^3/m_\chi^3)$, where $M_{\rm pl} = 1.22\times 10^{19}$ GeV denotes the Planck mass [11,13,20]. To summarize, for dark core collapse, the total number of captured DM particles inside a stellar object within its lifetime ($t_{\rm age}$) has to satisfy the following [11,13,20,24]

$$N_\chi|_{t_{\rm age}} = C\times t_{\rm age} \geq \max\,[N_\chi^{\rm self}, N_\chi^{\rm cha}]. \tag{6}$$

Note that, for stellar objects with high core temperature (such as Sun), the dark core collapse is essentially determined by $N_\chi^{\rm self}$ for bosonic as well as fermionic DM, leading to identical exclusion limits for bosonic/fermionic DM. Whereas, for stellar objects with low core temperature, the dark core collapse is determined by $N_\chi^{\rm self}$ ($N_\chi^{\rm cha}$) for bosonic (fermionic) DM, leading to distinct exclusion limits for bosonic/fermionic DM.

D. Growth and evaporation of nascent black holes

It is important to stress that dark core collapse does not ensure the successful transmutation of the hosts. If the nascent BH is sufficiently light, transmutation can cease for two different reasons. First, lighter BH takes a much longer time to swallow the hosts, and the swallow time ($\tau_{\rm swallow}$) can even be larger than the lifetime of the hosts. Second, and, more importantly, Hawking radiation becomes significant for lighter BH masses ($\sim 1/M_{\rm BH}^2$), causing a rapid evaporation of the nascent BH. Since the mass of the nascent BH becomes smaller for heavier DM mass, this provides an upper limit on DM mass that can be probed via transmutation [11,13,20,24]. We quantify the upper limits of m_χ for several stellar objects in the following, and it ranges around $\mathcal{O}(10^{10})$ GeV for the stellar objects under consideration.

For the time evolution of the nascent BH, we conservatively consider the baryonic matter accretion from the host (ignoring the possible DM accretion by the nascent BH) [11,13,50]

$$\frac{dM_{\rm BH}}{dt} = \frac{4\pi\rho_{\rm core}G^2M_{\rm BH}^2}{c_s^3} - \frac{P(M_{\rm BH})}{G^2M_{\rm BH}^2}, \tag{7}$$

where $c_s = \sqrt{T_{\rm core}/m_n}$ denotes the sound speed at the core of the stellar object, and $P(M_{\rm BH})$ denotes the Page factor [51,52]. Page factor properly accounts into gray-body corrections of the Hawking evaporation spectrum,

[1]This self-gravitating criterion is essentially equivalent to the Jeans instability criterion in Ref. [31] up to $\mathcal{O}(1)$ factors.

as well as the number of Standard Model (SM) species emission from an evaporating BH. In the classical black-body radiation limit, the Page factor evaluates to $1/(15360\pi)$, and is commonly used in the literature.

Considering the gray-body corrections, the Page factor can be written as $2.8\times10^{-4}f(M_{\rm BH})$, where $f(M_{\rm BH})$ encodes the number of SM species emission from an evaporating BH [52]. For $M_{\rm BH}\geq10^{17}$ g (which only emit massless particles, such as photons and neutrinos), $f(M_{\rm BH})$ is normalized to unity [52], and therefore, Page factor evaluates to $1/(1135\pi)$, an order of magnitude larger than the classical black-body limit. For $M_{\rm BH}\leq10^{17}$ g, the number of SM species emission from an evaporating BH crucially depends on its temperature (mass), and hence, $f(M_{\rm BH})$ varies with BH mass. We use the semi-analytic form of $f(M_{\rm BH})$ from Ref. [52] to estimate the Page factor in this regime. Quantitatively, for light BHs, i.e., $M_{\rm BH}\leq10^{10}$ g, which can emit all SM species, $f(M_{\rm BH})$ evaluates to 15.35, and for 10^{15} g $\leq M_{\rm BH}\leq10^{17}$ g (which can emit electrons, positrons, photons, and neutrinos), $f(M_{\rm BH})$ evaluates to 1.569. To summarize, depending on BH mass, $f(M_{\rm BH})$ ranges from (1–15.35), implying the range of Page factor from $1/(1135\pi)$ to $1/(74\pi)$. We verify that the Page factor obtained from the semi-analytic form of $f(M_{\rm BH})$ from Ref. [52] is in excellent agreement with the publicly available BLACKHAWK package [53].

Since, the accretion term scales as $M_{\rm BH}^2$, and the evaporation term scales as $1/M_{\rm BH}^2$, for low BH masses, evaporation dominates over the accretion process. Quantitatively, for the Sun, Jupiter, Earth, and moon, Hawking evaporation dominates over the Bondi-Hoyle accretion for

$$m_\chi\geq\begin{cases}7.1\times10^{11}\ \text{GeV}\\ 6.2\times10^{9}\ \text{GeV}\\ 2.4(5.3)\times10^{9}\ \text{GeV}\\ 1.0(6.0)\times10^{9}\ \text{GeV}\end{cases}\tag{8}$$

for nonannihilating bosonic (fermionic) DM. On the other hand, by requiring that the $\tau_{\rm swallow}$ has to be less than 1 Gyr, we obtain

$$m_\chi\geq\begin{cases}2.1\times10^{10}\ \text{GeV}\\ 1.1\times10^{10}\ \text{GeV}\\ 0.9(1.5)\times10^{10}\ \text{GeV}\\ 0.8(3.1)\times10^{10}\ \text{GeV}\end{cases}\tag{9}$$

for nonannihilating bosonic (fermionic) DM. We note that, for stellar objects with high core temperature, $\tau_{\rm swallow}$ essentially determines the washout of the transmutation, whereas, for stellar objects with low core temperature, it is determined by the efficient Hawking evaporation. This can simply be explained by the following. For high core-temperature stellar objects, the nascent BH becomes relatively larger ($M_{\rm BH,init}\sim T^{3/2}$), and therefore, the effects of Hawking evaporation become relatively subdominant, implying that accretion determines the termination of the transmutation.

E. Drift time and maximal possible scattering cross section

Transmutation of stellar objects also ceases at very high DM-nucleon scattering cross sections. This is simply because, at very high DM-nucleon cross sections, DM particles lose a significant amount of energy in the outer shells of these stellar objects and might not reach the stellar core to form a micro BH. In other words, the viscous drag force that drives the DM particles toward the core results in a long drift time, and therefore, prohibits transmutation. We estimate the drift time by using the stellar density, temperature, and compositional profiles [8,31,54]

$$t_{\rm drift}=\frac{1}{Gm_\chi}\sum_j\sigma_{\chi j}\int_0^R\frac{n_j(r)\sqrt{3A_jT(r)}}{\int_0^r d^3r'\rho_j(r')}dr,\tag{10}$$

where $\sigma_{\chi j}$ denotes the DM-nuclei scattering cross section, and it is related to the DM-nucleon scattering cross section via $\sigma_{\chi j}=\sigma_{\chi n}A_j^2(\mu_{\chi A_j}/\mu_{\chi n})^2$ with A_j is the mass number of the jth nuclei, and $\mu_{\chi n}$ is the reduced mass of the DM-nucleon system. We determine the ceilings of our results by demanding that $t_{\rm drift}\leq1$ Gyr. Quantitatively, for the (Sun) Earth, it corresponds to

$$\sigma_{\chi n}\leq(10^{-17})10^{-21}\ \text{cm}^2\left(\frac{m_\chi}{10^7\ \text{GeV}}\right),\tag{11}$$

and is same for bosonic/fermionic DM.

F. Properties of stellar objects

We accurately estimate the capture rate and the transmutation criterion for these stellar objects by utilizing stellar object properties, such as density profiles, temperature profiles, and detailed chemical compositions. In the following, we provide the inputs that have been considered for this analysis. The density and temperature profiles for the Sun, Earth, and Jupiter, which have been used in this analysis have also complied in Ref. [49].

(1) Sun: We use the solar density and temperature profiles from [55]. For the chemical composition, we assume that the Sun is entirely made up of ^{1}H [49].
(2) Jupiter: We use the Jupiter density and temperature profiles from the Jovian model J11-4a [56]. For the chemical composition, we assume that Jupiter is entirely made up of ^{1}H [49].
(3) Earth: We use the preliminary reference Earth model from [57] for the density profile, and we take the temperature profile from [58] under the assumption

of a hydrostatic equilibrium. For the chemical composition, we use the tabulated values from Ref. [54] with the core-mantle boundary at 3480 km, and the mantle-crust boundary at 6346 km. The core is dominantly made up of ^{56}Fe, whereas the mantle and the crust are dominantly made up of ^{16}O.

(4) Moon: We use the MAX model for density and the chemical compositions of the moon [59]. We take the lunar core-mantle boundary at 450 km, and the mantle-crust boundary at 1650 km. The lunar core is dominantly made up of ^{56}Fe, whereas the mantle and the crust is dominantly made up of ^{16}O. For the temperature profile, we consider the moon as an isothermal sphere with $T = 1700$ K [59].

It is important to stress that the interior modeling of the stellar objects considered in this analysis can have large uncertainties, and, depending on these uncertainties, the exclusion regions can vary. For the moon and Jupiter, the uncertainties are maximal [59–61], and it primarily affects the self-gravitating criterion, $N_\chi^{\rm self}$. Since the transmutation criterion for bosonic DM is determined by the self-gravitating criterion ($N_\chi^{\rm self}$), the exclusion regions for bosonic DM differ based on these uncertainties. Whereas, the exclusion regions remain unaltered for fermionic DM as the transmutation criterion for fermionic DM is essentially determined by the Chandrasekhar limit ($N_\chi^{\rm cha}$), which is independent of the internal modeling of the celestial objects. Quantitatively, for the moon, if we use the MIN model [59], we find that the exclusion region for bosonic DM weaken by a factor of $\sim$2 as compared to the result obtained from the MAX model.

III. RESULTS

We consider a variety of stellar objects, such as the Sun, Jupiter, the Earth, and the moon, and demonstrate their potential as nonannihilating DM detectors. These choices are well motivated by the fact they cover a wide range of size, density, and temperature, making them sensitive to different parts of the DM parameter space. Sun has the largest size and the highest core temperature, and as a consequence, the total number of captured DM particles as well as the threshold for transmutation both become higher. Jupiter has a somewhat larger size, but possesses a much lower core temperature, implying a higher capture rate but a lower threshold for transmutation. The Earth and moon have relatively smaller sizes and much lower core temperatures, and hence, the capture rate as well as the threshold for transmutation both becomes smaller.

We show our main results in Fig. 2 for nonannihilating bosonic and fermionic DM (spin-independent interactions). The top left (right) panel corresponds to Sun (Jupiter) as a DM detector, whereas, the bottom left (right) panel corresponds to the Earth (moon) as a DM detector. For stellar objects with low core temperatures, such as the moon, Earth, and Jupiter, the exclusion limit for bosonic DM is significantly stronger as compared to the fermionic DM. This is simply because for nonannihilating bosonic DM, the dark core collapse criterion is essentially determined by $N_\chi^{\rm self}$, whereas, for nonannihilating fermionic DM, it is determined by $N_\chi^{\rm cha}$, which is much higher than the self-gravitating criterion, i.e., $N_{\chi,\rm fermion}^{\rm cha} \gg N_\chi^{\rm self}$. This implies that transmutation for low core-temperature stellar objects is much harder to attain for nonannihilating fermionic DM, explaining the weaker exclusions. However, for stellar objects with higher core temperature, such as the Sun, the dark core collapse criterion for bosonic as well as fermionic DM is set by $N_\chi^{\rm self}$ (as it scales as $T_{\rm core}^{3/2}$), explaining identical exclusion limits for bosonic and fermionic DM.

The exclusion limits in Fig. 2 can be explained qualitatively from the following. For nonannihilating bosonic (fermionic) DM, the total number of captured DM particles linearly increases with lighter m_χ, whereas the threshold for transmutation increases as $m_\chi^{5/2}(m_\chi^3)$, and hence, for light DM masses, transmutation cannot be achieved. This explains the sharp vertical cutoffs in the low m_χ regime. For heavier DM masses, the mass of the nascent BH becomes smaller, resulting in two distinct effects. First, the nascent BH takes a substantially longer time to consume the host, and, second, Hawking evaporation becomes crucial. Because of these two effects, transmutation ceases, providing the vertical cutoffs around $m_\chi = 10^{10}$ GeV in Fig. 2. For the exact numerical values, see Sec. II D.

Next, we discuss the $\sigma_{\chi n}$ dependence of the exclusion limits in Fig. 2. For low DM-nucleon scattering cross sections, the total number of captured DM particles within the stellar objects decreases, and eventually falls below the threshold for transmutation, indicating that low $\sigma_{\chi n}$ cannot be probed via transmutation. Quantitatively, for nonannihilating bosonic DM, $\sigma_{\chi n} \leq 10^{-33}$ cm^2 ($\sigma_{\chi n} \leq 10^{-28}$ cm^2) cannot be probed by the existence of the Sun (Moon). Very high DM-nucleon scattering cross sections are also inaccessible via transmutations. This is simply because for very high $\sigma_{\chi n}$, the drift time of the DM particles becomes much longer, and they cannot reach the stellar core for large interactions. In Fig. 2, we show the ceilings of our results by demanding that $t_{\rm drift} \leq 1$ Gyr. For the Sun, it corresponds to $\sigma_{\chi n} \leq 10^{-17}$ cm^2 for $m_\chi = 10^7$ GeV, and linearly increases with heavier DM mass.

A. Comparison with the existing constraints

In Fig. 2, we show the existing constraints on spin-independent DM-nucleon scattering cross section (gray-shaded regions) for comparison. The existing constraints can be classified into three broad categories: astrophysical, cosmological, and terrestrial. Constraints obtained from the terrestrial direct detection experiments (labeled as

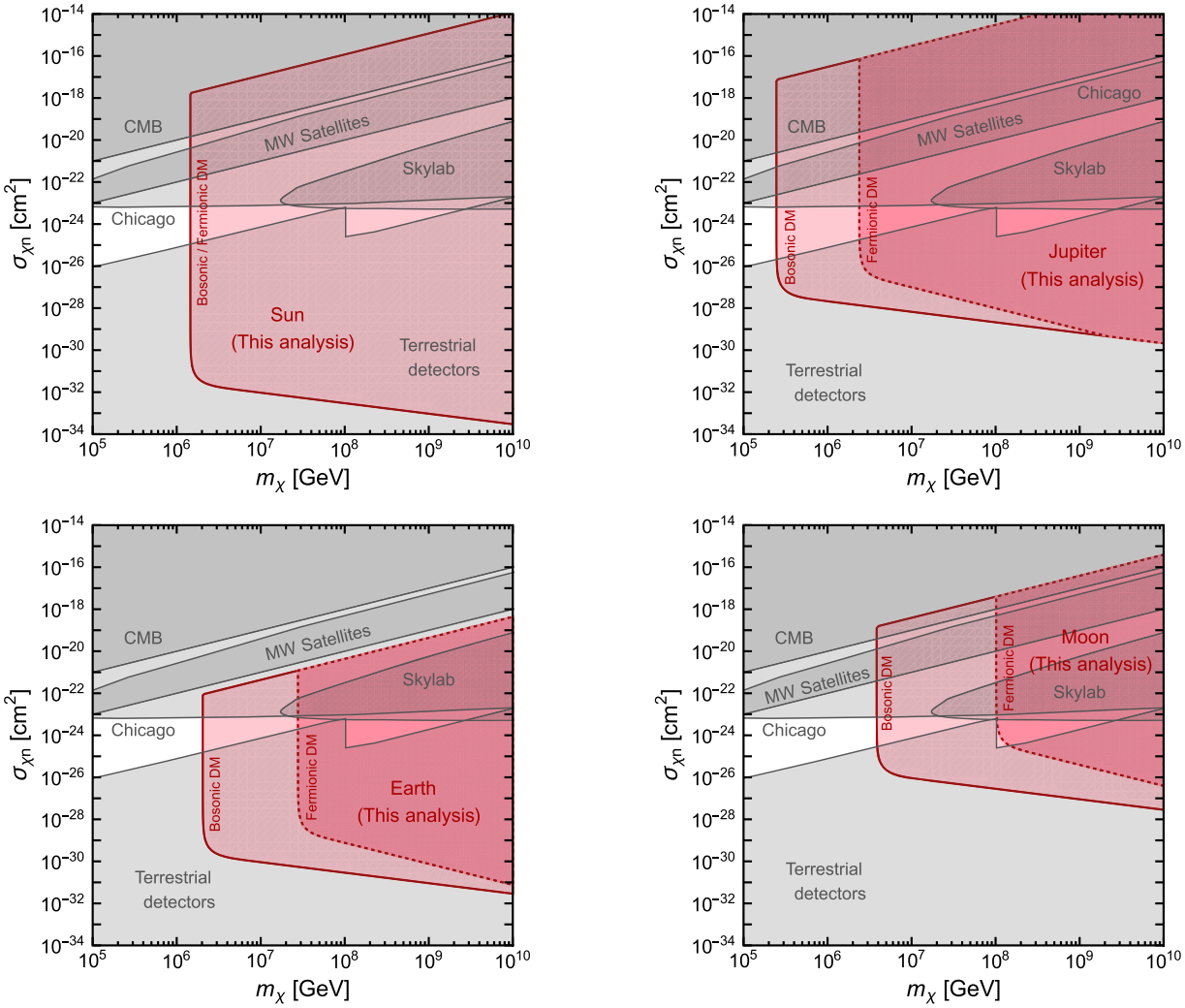

FIG. 2. Exclusion limits on spin-independent DM-nucleon scattering cross-sections from the existence of several stellar objects. The regions shaded by the solid red lines correspond to nonannihilating bosonic DM, whereas, the regions shaded by dashed red lines correspond to nonannihilating fermionic DM. The top left (right) panel corresponds to the Sun (Jupiter), whereas, the bottom left (right) panel corresponds to the Earth (moon). The existence of the stellar objects provides unprecedented sensitivity to strongly interacting heavy nonannihilating DM. We show the existing exclusion limits (gray shaded regions) from terrestrial searches [38–41] (collected in [42,62,63]), Skylab space station [64], a recent shallow-depth experiment carried out at University of Chicago [65], and cosmological measurements [34,36] for comparison. The existing constraints (gray-shaded regions) apply to both nonannihilating and annihilating DM, whereas, the constraints obtained from this analysis (red-shaded regions) apply solely to nonannihilating/very feebly annihilating DM.

terrestrial detectors) [38–41] are primarily based on the non observation of any anomalous scattering signature in the underground as well as in the surface detectors. We take these constraints from the summary plots in [42,62,63]. Cosmological constraints, such as Planck measurements of temperature and polarization anisotropy of the cosmic microwave background (labeled as CMB) [34,35], and Milky Way satellite observations (labeled as MW satellites) [36,37] are also shown for comparison. Astrophysical constraints, such as disk stability [29], interstellar gas cooling [66], and Galactic Center gas-cloud heating [67,68] are typically weaker than the constraints obtained from the Milky Way satellite observations, and therefore are not shown for clarity. Very recently, a shallow-depth experiment carried out at the University of Chicago (labeled as Chicago) [65] provides a stringent constraint on strongly interacting heavy DM, and we show it in Fig. 2. MAJORANA demonstrator at the Sanford underground research facility [69] and DEAP-3600 detector at SNOLAB [70] also provide exclusions on strongly interacting heavy DM interactions ($m_\chi \gtrsim 10^8$ GeV). However, since these exclusions do not cover any additional parameter space in Fig. 2, as compared to the "terrestrial detectors" [63], they are not shown. Large panels of etched plastic,

situated aboard the Skylab Space Station provide novel exclusion limits on DM-nucleon interactions (labeled as Skylab) [29,64,71]. Rocket-based x-ray quantum calorimetry (XQC) experiment [72], and searches for DM tracks in ancient underground mica [73,74] probe strongly-interacting heavy DM. However, the x-ray quantum calorimetry limit and the mica limit primarily apply for $m_\chi \leq 10^5$ GeV and $m_\chi \geq 10^{10}$ GeV, respectively, and hence, are not shown. Finally, constraints obtained from cosmic ray silicon detector satellite (IMP7/8), and balloon-borne experiment (IMAX) [71] are not based on detailed analyses in peer-reviewed papers, and therefore, are not shown in Fig. 2.

Comparing with the existing exclusion limits, it is evident that the existence of a variety of stellar objects provides novel constraints on strongly interacting heavy nonannihilating DM. It provides unprecedented sensitivity to some regions in the parameter space as compared to the existing searches. Quantitatively, the existence of the stellar objects exclude $\sigma_{\chi n} = 10^{-24}$ cm^2 for $m_\chi = 10^7$ GeV, not ruled by any other probes. This leading sensitivity simply stems from the fact that stellar objects, owing to their gigantic size and long lifetime, can capture a copious amount of Galactic DM particles for sufficiently high $\sigma_{\chi n}$, eventually causing an implosion. We note that, stellar objects with relatively larger sizes with much lower core temperatures, such as Jupiter, are the optimal targets to probe transmutation. This is simply because the total number of accumulated DM particles quadratically increases with a larger radius, and the threshold for transmutation falls off with lower core temperature, implying the most favorable transmutation criterion. It is also important to stress that the existing constraints from cosmological and terrestrial searches apply for both nonannihilating and annihilating DM interactions as they are solely based on scatterings. Whereas, the constraints obtained in this analysis apply only to nonannihilating/very-feebly annihilating DM particles.

We also note that, the exclusions obtained in Ref. [31] for the Earth are weaker than our analysis, however for the Sun, the constraints are similar. This can be explained in the following. Reference [31] derived their results for bosonic DM with non-negligible (repulsive) quartic self-interactions. Because of the repulsive self-interactions among the DM particles, the effective Chandrasekhar limit substantially increases [14], and it essentially determines the dark core collapse criterion for Earth. Whereas, in our analysis, we consider nonannihilating bosonic DM, and the dark core collapse criterion for Earth is determined by $N_\chi^{\rm self}$, explaining the difference between the two analyses. For the Sun, because of its much larger core temperature, $N_\chi^{\rm self}(\sim T_{\rm core}^{3/2})$ always exceeds over the Chandrasekhar limit and sets the dark core collapse criterion, resulting in a similar exclusion in both the analyses. For attractive self-interactions among the DM particles, bound-state formation occurs that affects the dynamics of dark core collapse [14,75,76].

B. Anomalous heating signatures

Nonannihilating DM can also heat up the stellar objects via successive scatterings with the stellar nuclei while getting captured. Such anomalous heating, commonly known as dark kinetic heating, can be observed in neutron stars with very low surface temperatures [77]. Cold neutron stars ($T_{\rm NS} = \mathcal{O}(1000)$ K) are ideal targets to search for dark kinetic heating as they have much higher escape velocities. Because of the large escape velocities, the velocity of the incoming DM particles gets significantly enhanced while falling into the steep gravitational potential of the neutron stars, and hence, they can transfer their kinetic energy to the stellar nuclei via collisions, heating up the cold neutron stars. We estimate the same for noncompact objects, concluding that because of their sufficiently low escape velocity, and larger size, such anomalous heating signatures are too low to observe.

IV. SUMMARY AND CONCLUSION

Celestial objects, owing to their enormous size and long lifetime, naturally act as novel DM detectors. We demonstrate that the continued existence of the Sun, Jupiter, Earth, and moon provides stringent constraints on strongly interacting nonannihilating DM interactions over a wide mass range. These choices are well motivated by the fact that each of these stellar objects (except the moon, which does not probe any additional parameter space as compared to Jupiter and the Sun because of its much smaller size) is an optimal detector in a different regime as they cover a different range of size, density, and temperatures. We probe regions in the DM parameter space, which are entirely inaccessible to the existing DM searches, demonstrating the novelty of our analysis. Our proposal is simply based on the fact that nonannihilating DM particles from the Galactic halo get captured inside the stellar objects if they interact sufficiently with the nucleons. For heavy DM, these captured DM particles rapidly thermalize within a very small region around the stellar core, resulting in a tantalizingly large core density. Once the core density exceeds its critical threshold value, nascent BH forms inside the stellar core, eventually destroying the hosts. The mere existence of these stellar objects excludes such DM mass and cross sections that predict the successful destruction of the hosts. We consider several stellar objects to demonstrate their potential as DM detectors and conclude that stellar objects with relatively larger sizes and low core temperatures, such as Jupiter, can probe the maximal DM mass window. Heavier DM masses are the most optimal for transmutation. However, as the nascent BH becomes smaller with an increase in DM mass, accretion becomes inefficient, and

the Hawking evaporation becomes crucial, ceasing the transmutation for heavy DM masses. Overall, given these stringent exclusion limits, our work naturally inspires similar analysis for other celestial objects, such as brown dwarfs, red giants, and exoplanets, once we have a better understanding of their density, temperature, and compositional properties. Finally, we point out an intriguing direction that the transmutation of celestial objects can lead to planetary mass BHs, possibly explaining the six ultrashort microlensing events observed in the OGLE data [78], NANOGrav detection of stochastic GW background [79], as well as the BH hypothesis of Planet-9 [80]. Since planet mass primordial BHs provide the viable solutions to this anomalies [78–80], it would be interesting to explore the alternative solutions via transmutation.

ACKNOWLEDGMENTS

It is my pleasure to thank Basudeb Dasgupta for helpful discussions and useful comments on the manuscript. I also thank Javier F. Acevedo, Sulagna Bhattacharya, Nirmal Raj, Rebecca Leane, Maxim Pospelov, and Juri Smirnov for helpful exchanges. A. R. acknowledges support from the National Science Foundation (Grant No. PHY-2020275) and from the Heising-Simons Foundation (Grant No. 2017-228).

[1] N. Aghanim *et al.* (Planck Collaboration), Planck 2018 results. VI. Cosmological parameters, Astron. Astrophys. **641**, A6 (2020).
[2] J. Cooley *et al.*, Report of the Topical Group on Particle Dark Matter for Snowmass 2021, arXiv:2209.07426.
[3] K. K. Boddy *et al.*, Snowmass2021 theory frontier white paper: Astrophysical and cosmological probes of dark matter, J. High Energy Astrophys. **35**, 112 (2022).
[4] W. H. Press and D. N. Spergel, Capture by the sun of a galactic population of weakly interacting, massive particles, Astrophys. J. **296**, 679 (1985).
[5] A. Gould, WIMP distribution in and evaporation from the sun, Astrophys. J. **321**, 560 (1987).
[6] A. Gould, Resonant enhancements in WIMP capture by the earth, Astrophys. J. **321**, 571 (1987).
[7] I. Goldman and S. Nussinov, Weakly interacting massive particles and neutron stars, Phys. Rev. D **40**, 3221 (1989).
[8] A. Gould, B. T. Draine, R. W. Romani, and S. Nussinov, Neutron stars: Graveyard of charged dark matter, Phys. Lett. B **238**, 337 (1990).
[9] G. Bertone and M. Fairbairn, Compact stars as dark matter probes, Phys. Rev. D **77**, 043515 (2008).
[10] A. de Lavallaz and M. Fairbairn, Neutron stars as dark matter probes, Phys. Rev. D **81**, 123521 (2010).
[11] S. D. McDermott, H.-B. Yu, and K. M. Zurek, Constraints on scalar asymmetric dark matter from black hole formation in neutron stars, Phys. Rev. D **85**, 023519 (2012).
[12] C. Kouvaris and P. Tinyakov, Constraining asymmetric dark matter through observations of compact stars, Phys. Rev. D **83**, 083512 (2011).
[13] C. Kouvaris and P. Tinyakov, Excluding Light Asymmetric Bosonic Dark Matter, Phys. Rev. Lett. **107**, 091301 (2011).
[14] N. F. Bell, A. Melatos, and K. Petraki, Realistic neutron star constraints on bosonic asymmetric dark matter, Phys. Rev. D **87**, 123507 (2013).
[15] T. Güver, A. E. Erkoca, M. Hall Reno, and I. Sarcevic, On the capture of dark matter by neutron stars, J. Cosmol. Astropart. Phys. 05 (2014) 013.
[16] J. Bramante, K. Fukushima, and J. Kumar, Constraints on bosonic dark matter from observation of old neutron stars, Phys. Rev. D **87**, 055012 (2013).
[17] J. Bramante, K. Fukushima, J. Kumar, and E. Stopnitzky, Bounds on self-interacting fermion dark matter from observations of old neutron stars, Phys. Rev. D **89**, 015010 (2014).
[18] C. Kouvaris and P. Tinyakov, Growth of black holes in the interior of rotating neutron stars, Phys. Rev. D **90**, 043512 (2014).
[19] J. Bramante and T. Linden, Detecting Dark Matter with Imploding Pulsars in the Galactic Center, Phys. Rev. Lett. **113**, 191301 (2014).
[20] R. Garani, Y. Genolini, and T. Hambye, New analysis of neutron star constraints on asymmetric dark matter, J. Cosmol. Astropart. Phys. 05 (2019) 035.
[21] C. Kouvaris, P. Tinyakov, and M. H. G. Tytgat, Non-Primordial Solar Mass Black Holes, Phys. Rev. Lett. **121**, 221102 (2018).
[22] B. Dasgupta, A. Gupta, and A. Ray, Dark matter capture in celestial objects: Light mediators, self-interactions, and complementarity with direct detection, J. Cosmol. Astropart. Phys. 10 (2020) 023.
[23] G.-L. Lin and Y.-H. Lin, Analysis on the black hole formations inside old neutron stars by isospin-violating dark matter with self-interaction, J. Cosmol. Astropart. Phys. 08 (2020) 022.
[24] B. Dasgupta, R. Laha, and A. Ray, Low Mass Black Holes from Dark Core Collapse, Phys. Rev. Lett. **126**, 141105 (2021).
[25] V. Takhistov, G. M. Fuller, and A. Kusenko, Test for the Origin of Solar Mass Black Holes, Phys. Rev. Lett. **126**, 071101 (2021).
[26] R. Garani, D. Levkov, and P. Tinyakov, Solar mass black holes from neutron stars and bosonic dark matter, Phys. Rev. D **105**, 063019 (2022).
[27] H. Steigerwald, V. Marra, and S. Profumo, Revisiting constraints on asymmetric dark matter from collapse in white dwarf stars, Phys. Rev. D **105**, 083507 (2022).

[28] D. Singh, A. Gupta, E. Berti, S. Reddy, and B. S. Sathyaprakash, Constraining properties of asymmetric dark matter candidates from gravitational-wave observations, arXiv:2210.15739.
[29] G. D. Starkman, A. Gould, R. Esmailzadeh, and S. Dimopoulos, Opening the window on strongly interacting dark matter, Phys. Rev. D **41**, 3594 (1990).
[30] Y. Kurita and H. Nakano, Gravitational waves from dark matter collapse in a star, Phys. Rev. D **93**, 023508 (2016).
[31] J. F. Acevedo, J. Bramante, A. Goodman, J. Kopp, and T. Opferkuch, Dark matter, destroyer of worlds: Neutrino, thermal, and existential signatures from black holes in the sun and earth, J. Cosmol. Astropart. Phys. 04 (2021) 026.
[32] R. K. Leane and J. Smirnov, Exoplanets as Sub-GeV Dark Matter Detectors, Phys. Rev. Lett. **126**, 161101 (2021).
[33] R. K. Leane and T. Linden, First analysis of jupiter in gamma rays and a new search for dark matter, arXiv:2104.02068.
[34] V. Gluscevic and K. K. Boddy, Constraints on Scattering of keV–TeV Dark Matter with Protons in the Early Universe, Phys. Rev. Lett. **121**, 081301 (2018).
[35] K. K. Boddy, V. Gluscevic, V. Poulin, E. D. Kovetz, M. Kamionkowski, and R. Barkana, Critical assessment of CMB limits on dark matter-baryon scattering: New treatment of the relative bulk velocity, Phys. Rev. D **98**, 123506 (2018).
[36] E. O. Nadler *et al.* (DES Collaboration), Milky Way Satellite Census. III. Constraints on Dark Matter Properties from Observations of Milky Way Satellite Galaxies, Phys. Rev. Lett. **126**, 091101 (2021).
[37] E. O. Nadler, V. Gluscevic, K. K. Boddy, and R. H. Wechsler, Constraints on dark matter microphysics from the milky way satellite population, Astrophys. J. Lett. **878**, 32 (2019).
[38] E. Aprile *et al.* (XENON Collaboration), First Dark Matter Search Results from the XENON1T Experiment, Phys. Rev. Lett. **119**, 181301 (2017).
[39] G. Angloher *et al.* (CRESST Collaboration), Results on MeV-scale dark matter from a gram-scale cryogenic calorimeter operated above ground, Eur. Phys. J. C **77**, 637 (2017).
[40] A. H. Abdelhameed *et al.* (CRESST Collaboration), First results from the CRESST-III low-mass dark matter program, Phys. Rev. D **100**, 102002 (2019).
[41] D. Abrams *et al.* (CDMS Collaboration), Exclusion limits on the WIMP nucleon cross-section from the cryogenic dark matter search, Phys. Rev. D **66**, 122003 (2002).
[42] B. J. Kavanagh, Earth scattering of superheavy dark matter: Updated constraints from detectors old and new, Phys. Rev. D **97**, 123013 (2018).
[43] J. Bramante, J. Kumar, G. Mohlabeng, N. Raj, and N. Song, Light dark matter accumulating in terrestrial planets: Nuclear scattering, arXiv:2210.01812.
[44] D. A. Neufeld, G. R. Farrar, and C. F. McKee, Dark matter that interacts with baryons: Density cistribution within the earth and new constraints on the interaction cross-section, Astrophys. J. **866**, 111 (2018).
[45] B. Bertoni, A. E. Nelson, and S. Reddy, Dark matter thermalization in neutron stars, Phys. Rev. D **88**, 123505 (2013).
[46] R. Garani, A. Gupta, and N. Raj, Observing the thermalization of dark matter in neutron stars, Phys. Rev. D **103**, 043019 (2021).
[47] A. Gould and G. Raffelt, Thermal conduction of massive particles, Astrophys. J. **352**, 654 (1990).
[48] H. Banks, S. Ansari, A. C. Vincent, and P. Scott, Simulation of energy transport by dark matter scattering in stars, J. Cosmol. Astropart. Phys. 04 (2022) 002.
[49] R. K. Leane and J. Smirnov, Floating dark matter in celestial bodies, arXiv:2209.09834.
[50] R. Garani and S. Palomares-Ruiz, Dark matter in the sun: Scattering off electrons vs nucleons, J. Cosmol. Astropart. Phys. 05 (2017) 007.
[51] D. N. Page, Particle emission rates from a black hole: Massless particles from an uncharged, nonrotating hole, Phys. Rev. D **13**, 198 (1976).
[52] J. H. MacGibbon, Quark and gluon jet emission from primordial black holes. 2. The lifetime emission, Phys. Rev. D **44**, 376 (1991).
[53] A. Arbey and J. Auffinger, Physics beyond the Standard Model with BlackHawk v2.0, Eur. Phys. J. C **81**, 910 (2021).
[54] J. Bramante, A. Buchanan, A. Goodman, and E. Lodhi, Terrestrial and martian heat flow limits on dark matter, Phys. Rev. D **101**, 043001 (2020).
[55] J. Christensen-Dalsgaard, W. Dappen, S. V. Ajukov, E. R. Anderson, H. M. Antia, S. Basu *et al.*, The current state of solar modeling, Science **272**, 1286 (1996).
[56] M. French, A. Becker, W. Lorenzen, N. Nettelmann, M. Bethkenhagen, J. Wicht, and R. Redmer, Ab Initio simulations for material properties along the Jupiter Adiabat, Astrophys. J. Suppl. Ser. **202**, 5 (2012).
[57] A. M. Dziewonski and D. L. Anderson, Preliminary reference earth model, Phys. Earth Planet. Interiors **25**, 297 (1981).
[58] Y. Zhang, J.-F. Lin, H. He, F. Liu, M. Zhang, T. Sato *et al.*, Shock compression and melting of an fe-ni-si alloy: Implications for the temperature profile of the earth's core and the heat flux across the core-mantle boundary, J. Geophys. Res. Solid Earth **123** (2018).
[59] R. Garani and P. Tinyakov, Constraints on dark mtter from the moon, Phys. Lett. B **804**, 135403 (2020).
[60] N. Nettelmann, A. Becker, B. Holst, and R. Redmer, Jupiter models with improved *Ab Initio* hydrogen equation of state (H-REOS.2), Astrophys. J. **750**, 52 (2012).
[61] Y. Miguel, T. Guillot, and L. Fayon, Jupiter internal structure: The effect of different equations of state, Astron. Astrophys. **596**, A114 (2016).
[62] M. C. Digman, C. V. Cappiello, J. F. Beacom, C. M. Hirata, and A. H. G. Peter, Not as big as a barn: Upper bounds on dark matter-nucleus cross sections, Phys. Rev. D **100**, 063013 (2019).
[63] D. Carney *et al.*, Snowmass2021 Cosmic Frontier White Paper: Ultraheavy Particle Dark Matter, arXiv:2203.06508.
[64] A. Bhoonah, J. Bramante, B. Courtman, and N. Song, Etched plastic searches for dark matter, Phys. Rev. D **103**, 103001 (2021).
[65] C. V. Cappiello, J. I. Collar, and J. F. Beacom, New experimental constraints in a new landscape for composite dark matter, Phys. Rev. D **103**, 023019 (2021).

[66] R. S. Chivukula, A. G. Cohen, S. Dimopoulos, and T. P. Walker, Bounds on Halo Particle Interactions From Interstellar Calorimetry, Phys. Rev. Lett. **65**, 957 (1990).

[67] A. Bhoonah, J. Bramante, F. Elahi, and S. Schon, Calorimetric Dark Matter Detection With Galactic Center Gas Clouds, Phys. Rev. Lett. **121**, 131101 (2018).

[68] A. Bhoonah, J. Bramante, S. Schon, and N. Song, Detecting composite dark matter with long-range and contact interactions in gas clouds, Phys. Rev. D **103**, 123026 (2021).

[69] M. Clark, A. Depoian, B. Elshimy, A. Kopec, R. F. Lang, and J. Qin, Direct detection limits on heavy dark matter, Phys. Rev. D **102**, 123026 (2020).

[70] P. Adhikari *et al.* (DEAP Collaboration), First Direct Detection Constraints on Planck-Scale Mass Dark Matter with Multiple-Scatter Signatures Using the DEAP-3600 Detector, Phys. Rev. Lett. **128**, 011801 (2022).

[71] B. D. Wandelt, R. Dave, G. R. Farrar, P. C. McGuire, D. N. Spergel, and P. J. Steinhardt, Selfinteracting dark matter, in *4th International Symposium on Sources and Detection of Dark Matter in the Universe (DM 2000)* (2000), pp. 263–274, arXiv:astro-ph/0006344.

[72] A. L. Erickcek, P. J. Steinhardt, D. McCammon, and P. C. McGuire, Constraints on the interactions between dark matter and baryons from the X-ray quantum calorimetry experiment, Phys. Rev. D **76**, 042007 (2007).

[73] P. B. Price and M. H. Salamon, Search for Supermassive Magnetic Monopoles Using Mica Crystals, Phys. Rev. Lett. **56**, 1226 (1986).

[74] J. Bramante, B. Broerman, J. Kumar, R. F. Lang, M. Pospelov, and N. Raj, Foraging for dark matter in large volume liquid scintillator neutrino detectors with multi-scatter events, Phys. Rev. D **99**, 083010 (2019).

[75] M. I. Gresham and K. M. Zurek, Asymmetric dark stars and neutron star stability, Phys. Rev. D **99**, 083008 (2019).

[76] R. Garani, M. H. G. Tytgat, and J. Vandecasteele, Condensed dark matter with a Yukawa interaction, Phys. Rev. D **106**, 116003 (2022).

[77] M. Baryakhtar, J. Bramante, S. W. Li, T. Linden, and N. Raj, Dark Kinetic Heating of Neutron Stars and An Infrared Window On WIMPs, SIMPs, and Pure Higgsinos, Phys. Rev. Lett. **119**, 131801 (2017).

[78] H. Niikura, M. Takada, S. Yokoyama, T. Sumi, and S. Masaki, Constraints on earth-mass primordial black holes from OGLE 5-year microlensing events, Phys. Rev. D **99**, 083503 (2019).

[79] G. Domènech and S. Pi, NANOGrav hints on planet-mass primordial black holes, Sci. China Phys. Mech. Astron. **65**, 230411 (2022).

[80] J. Scholtz and J. Unwin, What if Planet 9 is a Primordial Black Hole?, Phys. Rev. Lett. **125**, 051103 (2020).